Available online at https://link.springer.com/journal/42241
http://www.jhydrodynamics.com
Journal of Hydrodynamics, 2022
https://doi.org/10.1007/s42241-022-0026-3

Research progress on the hydrodynamic performance of water-air-bubble mixed flows around a ship

Zheng Li, Xiao-song Zhang, De-cheng Wan*
Computational Marine Hydrodynamics Lab (CMHL), School of Naval Architecture, Ocean and Civil Engineering, Shanghai Jiao Tong University, Shanghai 200240, China

(Received January 22, 2022, Revised January 25, 2022, Accepted February 8, 2022, Published online April 27, 2022)

Abstract: The interaction between ship and surrounding fluids generates the water-air-bubble mixed flow laden with numerous droplets and bubbles. The water-air-bubble mixed flow is a complex multi-phase flow phenomenon, which involves intense air-water mixture, complex evolution of interface shape, interactions between multi-scale flow structures and strong turbulent fluctuations. Based on the field observations at sea, a large range of white water-air-bubble flow exists widely around a large-scale sailing ship, and directly affects the hydrodynamic performance of ship from various aspects. This paper reviews the research progress of water-air-bubble mixed flow around a ship. Current knowledge about the formation and evolution mechanism are introduced firstly. Then, the effects of the water-air-bubble mixed flow on ship performance are further reviewed, the main concerns are ship resistance, propulsion performance, slamming and maneuverability. Finally, the future research prospects are summarized.

Key words: Water-air-bubble mixed flow, ship resistance, propulsion performance, ship slamming characteristics, maneuverability

Corresponding authors' biography

Prof. De-cheng Wan is a distinguished professor of Shanghai Jiao Tong University (SJTU), chair professor of Chang Jiang Scholar, distinguished professor of Shanghai Eastern Scholar, Shanghai Excellent Academic Leader. He is awarded the most cited researchers in 2018, 2019, 2020, 2021 by Elsevier, and has delivered over 80 invited or keynote presentations in international conferences. He is Director of Computational Marine Hydrodynamics Lab (CMHL, https://dcwan.sjtu.edu.cn/), member of ISOPE Board of Directors, Chair of ISOPE International Hydrodynamic Committee, member of advisor committee of International Towing Tank Conference (ITTC), standing council member of Association of Global Chinese Computational Mechanics, Associate Editor-in-Chief of Journal of Hydrodynamics, and member of editorial board of Ocean Engineering and Applied Ocean Research. His research interest is mainly on computational marine and coastal hydrodynamics, numerical marine basin, nonlinear wave theory, wave loads on structures, numerical analysis of riser vortex-induced vibration (VIV) and platform vortex-induced motion (VIM), fluid-structure interaction, offshore wind turbine and other offshore renewable resources, etc. In these areas, he has published over 500 papers and carried out more than 50 projects on marine computational hydrodynamics. His remarkable works of development of numerical solvers in ship and ocean engineering have been recognized by the world-wide researchers in the field of marine hydrodynamics.

Project supported by the National Natural Science Foundation of China (Grant Nos. 52131102, 51879159), the National Key Research and Development Program of China (Grant No. 2019YFB1704200).
Biography: Zheng Li (1995-), Male, Ph. D. Candidate,
E-mail: u201312243@sjtu.edu.cn
Corresponding author: De-cheng Wan,
E-mail: dcwan@sjtu.edu.cn

Introduction

Interactions between navigating ships and free surface flow will generate a sort of white, water-air-bubble mixed flow (as shown in Fig. 1), which is much more significant around the high-speed and large-scale sailing ships. Intense splashing jets produced by the violent impact between wave and ship will break up into numerous satellite droplets, form a spray region over the two-phase interface. On the other hand, large air pockets or cavities are entrapped underwater due to the overturning of wave front, which will distort and fragment into air filaments and

multi-scale bubbles under strong turbulent shear. There are also strong mixture of bubbles or droplets near the violent deformed interface, which change the refraction and reflection characteristics of incident light. Therefore, the highly mixed two-phase flow usually appears as white, foam-like.

Fig. 1 (Color online) white water-air-bubble mixed flow around a sailing ship

The formation mechanisms and evolution process of water-air-bubble mixed flow differs in different regions around the ship. Near the bow, impact between the hull and surrounding fluid lead to the overturning and breaking of free surface, which will cause air entrainment underwater and subsequent splashing above the water surface. Near the midship, the water-air-bubble mixed flow on both sides will expand further and diffuse into the far field region away from the hull following the motion of bow wave. Behind the stern, the cavitation flow generated by the rotating propellers will interact with the separated wake flow. The process will enhance the flow instability, turbulence fluctuation and two-phase mixture, producing a large-scale, turbulent bubbly wake. These phenomena are different forms of water-air-bubble mixed flow around the ship, which are ubiquitous when considering the large-scale (or full-scale) problems. Although the water-air-bubble mixed flow are commonly observed, but there are no available theories or methods to describe and analyze the typical phenomenon mechanistically and systematically.

The water-air-bubble mixed flow has significant effects on the hydrodynamic performance of sailing ships from different aspects:

(1) Resistance: The large-scale water-air-bubble mixed flow is generated by the interaction between ship and surrounding fluid (Fig. 2(a)), which is often accompanied by the violent wave breaking and significant energy dissipation. The added resistance caused by energy dissipation will lead to the increasingly fuel consumption and pollutant emissions

(2) Propulsion performance: The intense air-liquid mixture induced by the water-air-bubble mixed flow near the stern lead to a non-uniform inlet flow from upstream (Fig. 2(b)), which may exacerbate the cavitation on the propeller blade and decrease the general propulsion efficiency.

(3) Sea-keeping: As introduced before, the water-air-bubble mixed flow usually appears as the spray flow containing numerous droplets or splashing jets over interface (Fig. 2(c)). The spatial distribution and magnitude of ship slamming loads will be changed, which directly affect the motion and dynamic response of ship, local structural strength and comfortability during sailing.

(a) Bow wave breaking and water-air-bubble mixed flow generated by high-speed warship

(b) The air bubbles mixing near the propeller

(c) Violent impact and spray flow during the ship slamming

(d) The two-phase mixed flow around the rudder and hull

Fig. 2 (Color online) Complex interaction between water-air-bubble mixed flow and the sailing ship

(4) Ship maneuverability: A real navigating ve-

ssel is usually a complex multi-system, which often consists of hull, propeller and rudder. The generation and evolution of water-air-bubble mixed flow around the multi-system is complex (Fig. 2(d)), which may interfere with the coupling between hull, propeller and rudder and increase the uncertainty for ship maneuverability.

(5) Others: Except for the canonical hydrodynamic performance of ship, it is also found that the dynamic behavior of bubble clouds (or droplet spray) enhances the turbulent fluctuation in the dispersed multiphase flow, which will change the flow-induced noise around marine structures and affect the signal transmission of acoustic detection equipment (e.g., sonar[1-4]). Besides, the large-scale bubbly wake laden with enormous bubbles and droplets is easy to detect and track due to enhanced acoustic or optical signal, which greatly reduces the stealth capability of war ship.

In summary, the water-air-bubble mixed flow around the ship is closely related to the design of advanced green ship, the development of energy saving technique, structural safety, vibration reduction and noise control. On the other hand, this problem involves the interaction of multi-phase, multi-scale structures and multi-system, which makes it a great challenge to discern what is happening mechanistically. The engineering and academic significance attract extensive attention of scholars, which has been a hot issue in the ship and ocean engineering. In this paper, the research progress of water-air-bubble mixed flow around the ship is reviewed. It is the purpose of this contribution to present the complicated features of the typical two-phase mixed flow commonly encountered in ship and ocean engineering. The main focuses lie in its influence on the performance of marine structures in various aspects. We begin with the generation and evolution of water-air-bubble mixed flow near the sailing ships. Then the influence of the water-air-bubble mixed flow is considered from four aspects: Resistance, propulsion, see-keeping and maneuverability. The relevant experimental and numerical studies will be summarized in detail. The last section discusses the future research prospects.

1. Generation and evolution of water-air-bubble mixed flow near the sailing ships

During the navigation of the ship, a wide range of water-air-bubble mixed flow will be generated around it. The multi-phase mixed flow varies greatly along the hull. The formation mechanism and evolution process are different near the bow, midship and stern due to the difference of the geometrical shape and installed equipment.

For a large-scale sailing ship, the bow wave is usually unstable and irregular, which is often accompanied by wave breaking and intense water-air mixture. Therefore, the problem of bow wave breaking is one of the main focuses. The classical experimental studies mainly focus on the morphological changes of the bow wave under different Froude numbers[5-7]. The Froude number in these model tests is generally in the range of 0.28-0.45. The main idea of the experiments is to produce the wave-breaking by increasing the towing speed of model. The high-speed camera is usually used to observe the process of wave breaking, capture the typical flow structures and record the locations of bow wave running-up. The Particle image velocimetry (PIV) technology can be employed to measure the velocity/pressure field and analyze the evolution of vortical flow field around the ship. Current studies[7] showed that the overturning of bow wave in the cases with high Froude numbers and subsequent splashing will produce significant air entrainment and droplets spray together, which account for the generation of water-air-bubble mixed flow around the bow.

Experimental techniques provide efficient means for understanding the phenomenological evolution and general flow characteristics of the bow wave. With computation fluid dynamics (CFD) tools, we can further identify the type and understand the nature of bow wave breaking. Most of the previous numerical studies are based on the Reynolds-averaged Navier-Stokes (RANS) equations[8-12], the largest Froude number in these studies is 0.62. The overturning of bow wave and jet splashing can be captured while details of the turbulent flow field cannot be resolved well due to the time-averaging perator. Therefore, the detached eddy simulation (DES) combined with volume of fluid (VOF) or level set method has been prevalent in the simulation of bow wave breaking[13-17], the Froude number has been raised to 1.2. From the predicted free surface flow field as showed in Fig. 3, the typical flow structures (e.g., overturning breaking of bow wave, subsequent jet splashing) can be reproduced well in the simulation. The wave profile, vorticity and velocity field at several transverse sections are used to explain the formation of secondary jets. It is found that the counter-rotating vortex pairs generated by the overturning wave hits the free surface will lead to the great velocity gradient in the transverse direction, which contribute most to the formation of secondary jets.

Present numerical studies can help us understand the formation of water-air-bubble mixed flow near bow. However, the transportation and dynamic behavior of multi-scale bubbles due to bow wave breaking cannot be resolved well due to the numerical dissipation and insufficient grid resolution away from the model. Therefore, high-fidelity simulation based

on high-order temporal/spatial discrete schemes and novel grid refinement technique is necessary for the intensive analysis of water-air-bubble mixed flows. Recently, Hu et al.[18] has performed the numerical simulation of breaking bow wave generated by a rectangular plate. The flow structures and bubble formation during the breaking process are under full quantitative investigation. The typical phenomenon of water-air-bubble mixed flow, including the break-up of thin liquid sheet, jet overturning and splash-ups are well reproduced by the present simulation (Fig. 4). Due to the use of adaptive mesh refinement technique, high-grid resolution can retain in the region with two-phase interface. Therefore, the evolution of bubble clouds in the downstream region can also be resolved and quantitatively analyzed. Although the test case is different from the bow wave breaking around a real ship model, the current studies have showed that the CFD tool is promising in the mechanical analysis of complex water-air-bubble mixed flow generated by a surface-piercing structure.

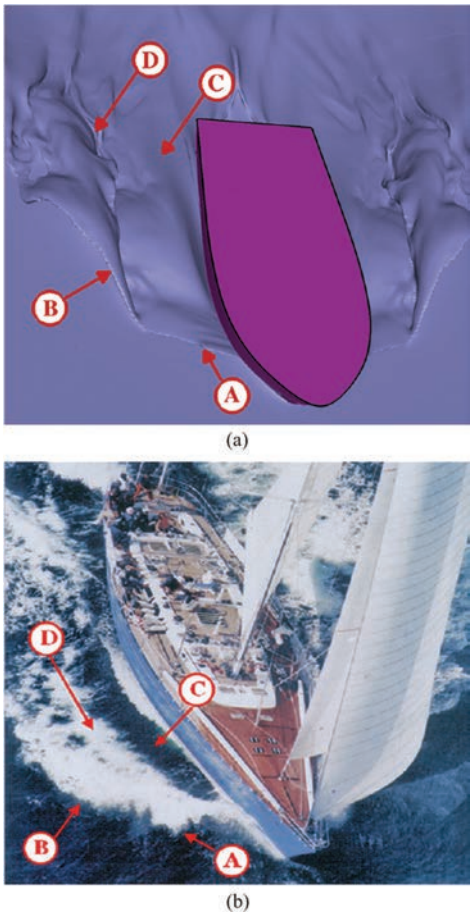

Fig. 3 (Color online) Comparison between numerical simulation and sea trial of water-air-bubble mixed flow induced by bow wave breaking[14]

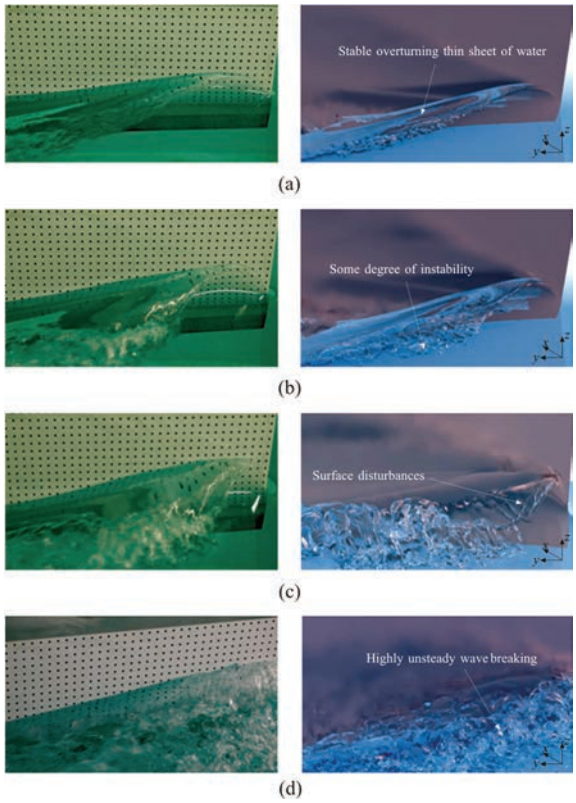

Fig. 4 (Color online) The bow waves generated by a rectangular plate with different yaw angles. The left-hand column indicates the experimental observation[19-20] and the right-hand pictures are simulation results[18]

The water-air-bubble mixed flow generated by bow wave breaking will further transport downstream and interact with the boundary layer flow near the midship. As mentioned above, the generation of water-air-bubble mixed flow at the model scale requires a high speed of ship model. The entrapped air bubbles are prone to rise under buoyancy and escape away from free surface. Therefore, it is difficult to study the evolution of water-air-bubble mixed flow at model scale. Johansen et al.[21-22] carried out valuable field observation studies. The bubble flow field around the Athena II ship was measured at full scale. A new technique for bubble measurement considering the probe size was used, the gas volume fraction, distribution of bubble velocity and size are obtained. It is found that the air entrainment is obviously enhanced with the increase of the ship speed. The average bubble velocity near the midship is slightly larger than the ship speed. The bubble velocity increases with depth and decreases inside the boundary layer. Near the free surface, the average bubble size is larger. Small bubbles will be transported along the hull bottom, which enter the transom flow. Some scholars[23] has proposed the phenomenological air entrainment model to predict

the bubbles around the surface ship based on the field observation. They studied the location and rate of air entrainment, discussed the differences of bubbly flow charac- teristics between straight ahead and turning motions. The numerical studies provide a basis for better understanding the physical processes of the interaction between water-air-bubble mixed flow with a surface ship. Since the number of entrapped air bubbles near the midship is very large, the accurate numerical prediction with prevalent interface capture method is nearly impossible. Therefore, the polydisperse two-fluid approach[24] seems to be a better choice in the analysis of the distribution and evolution of large-scale water-air-bubble mixed flow.

Behind the stern, the large-scale bubbly wake is the main concern, which is usually affected by the significant flow separation and disturbance of the propeller motion. In terms of field observation studies, some scholars focus on the large-scale features of wake. Peltzer et al.'s[25] early observations of wake flow behind the high-speed ships show the surface-active films generated by the passage of a surface ship will exist tens of kilometers downstream. Sonar technology can be used to obtain the shape of bubbly wake[26-27]. Soloviev et al.[26] used three-dimensional sonar technology to carry out the field observations on a vessel in the inland waterway, analyzed the difference of bubbly wake generate by free surface breaking and propeller rotation. The bubbly flow structures larger than centimeter scale can be reproduced as Fig. 5 presented.

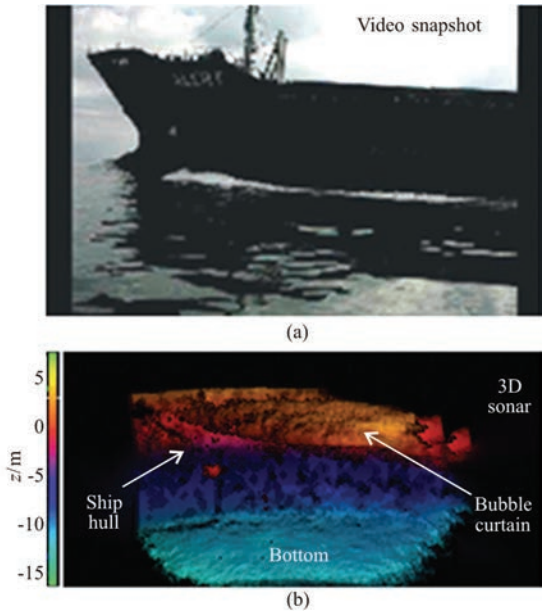

Fig. 5 (Color online) three-dimensional sonar view of the bubble cloud around hull and in the far-field wake[26]

The behavior of water-air-bubble mixed flow is highly correlated with the stern shape. Many scholars investigated the wake characteristics with the model test of a high-speed transom stern[28-30]. Shen et al.[28] used digital particle image velocimetry (DPIV) to measure the bubbly wake characteristics behind the different ship models. The two-phase turbulent flow field, including flow structures and turbulent statistical characteristics are analyzed in detail. The Naval Surface Warfare Center of United States has carried out high-speed towing tests of a large-scale transom-stern[29-30]. Several experimental techniques (e.g., high-speed photography, underwater videography, void fraction probes) are employed to depict the characteristics of water-air-bubble mixed flow from the perspectives of spatial distribution of void fraction, bubble number density and size distribution. The influence of towing speeds was also analyzed.

For the numerical researches, the unsteady Reynolds averaged[31] or large eddy simulation (LES)[32-33] have been used in the simulation of bubbly wake. Hendrickson et al.[32] present high-resolution implicit large eddy simulation (ILES) of turbulent bubbly wake behind three-dimensional transom sterns and the results have shown a similarity in the presence of shear layer region between the wake flow and canonical hydraulic jumps[34-38]. However, the presence of transom stern increases the complexness of two-phase flow phenomena and the flow features differs from a supercritical hydraulic jump[35, 39-40]. They have depicted flow structures in the mixed region and quantify the large-scale air entrainment behavior in the wake. Furthermore, a simple, regional explicit algebraic closure model for the turbulent mass flux (TMF) is developed based on high-resolution data of incompressible highly variable density turbulence (IHVDT) in the near surface mixed-phase region[33]. As the traditional fixed mesh refinement strategies require demanding computational cost even on high-performance computers (HPC), adaptive mesh refinement method[41-44] combined with high-order convection schemes[45] and high-robustness mass-momentum consistent advection algorithm[46-49] has been successfully used in the simulation of bubbly wake behind the transom stern as Fig. 6 presented. The multi-scale entrapped bubbles are mainly distributed in two regions: Near the wake centerline and the location where diverging wave breaks[50]. Also, the bubble size distribution follows well a canonical power-law[51-54] in Fig. 7 proves that the turbulent break-up is dominant for the bubbles formation.

2. The effect of water-air-bubble mixed flow on ship resistance

The traditional method for resistance prediction is based on the model-scale experimental test or numerical simulation. Then the measured resistance is

converted to full-scale according to empirical formula[55]. In traditional theory, the ship resistance can be divided into wave resistance, friction resistance, and viscous pressure resistance. The two-dimensional and three-dimensional method are established and extensively applied to predict the ship resistance. Some empirical coefficients (e.g., ΔCf , Ca) should be included in the conversion formula considering the full-scale effect. These empirical coefficients which are employed to modify the resistance contain three kinds of unclear effects: Scale effect, the effect of physical phenomenon that cannot be reproduced in the model test (e.g., the effect of wind velocity and hull roughness) and the coupling effect between different components of resistance. The water-air-bubble mixed flow around the ship is one of the typical problems of the second category. As shown in Fig. 8, under similar Froude number, there is almost no water-air-bubble mixed flow generated near the model[7, 56-57]. However, the white water-air-bubble mixed flow can be clearly identified around the full-scale ship. Therefore, the added drag induced by large-scale water-air-bubble mixed flow cannot be accurately considered in the current theory for resistance prediction, which also becomes one of the bottleneck problems in the design of high-speed ship.

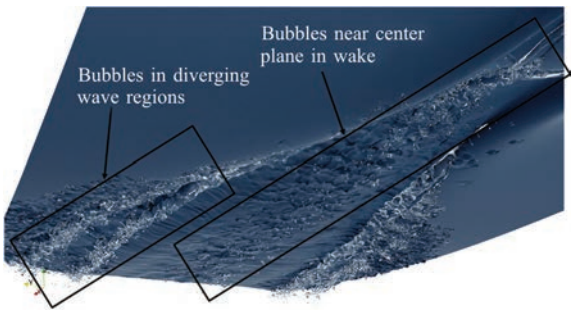

Fig. 6 (Color online) High-fidelity simulation of the bubbly wake behind a high-speed transom stern[50]

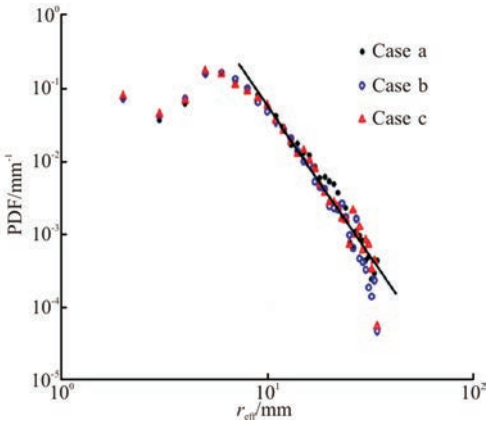

Fig. 7 (Color online) The size distribution of bubbles in the bubbly wake flow[50]

Fig. 8 (Color online) Comparison between the free surface flow field around the ship with model-scale (a) and full-scale (b)

The effect of water-air-bubble mixed flow on the ship resistance can be considered from different aspects. The generation of water-air-bubble mixed flow is accompanied by obvious momentum and energy transfer processes. The energy is initially transferred from the sailing ship to the surrounding fluid during the impact. As the water-air-bubble mixed flow is generated, the energy is successively transferred from the bulk volumes of water to the numerous droplets and bubbles. Therefore, small-scale bubbles or droplets can persist for a long time in the multi-phase mixed flow. The conversion of energy mainly consists of three parts: Firstly, the wave run up along the hull, which is followed by the overturning break of bow wave and subsequent splashing[58-59]. The elevated wave front and liquid splashing has large gravitational potential energy. Secondly, many entrained bubbles or splashing droplets move at high speed. Therefore, an appreciable portion of initial energy is converted to the kinetic energy. Thirdly, the original continuous water-air interface is broken into liquid (or air) filaments and numerous droplets (or bubbles), which significantly increase the surface energy. Except for the conversion between different components of energy, energy dissipation during to viscous effect and turbulence is also considerable and should not be ignored. The energy dissipation and conversion caused by the water-air-bubble mixed flow will lead to the increased ship resistance and fuel consumption.

Although there have been lots of experimental and numerical studies of the free-surface flow around

a surface-piercing structure[60-64], corresponding studies on the energy analysis especially for the water-air-bubble mixed flow around ship are rarely seen in the published literatures. Since the water-air-bubble mixed flow is mostly generated by the wave breaking process in different regions, studies related to wave breaking[59, 65-66] can be used for reference. The wave-breaking is responsible for the enhancement of energy dissipation and turbulent mixing near free surface[59, 67]. In the early stage of breaking, the energy of surface wave is lost due to gas entrainment and turbulent mixing. According to laboratory observations[67], about 40% of the total wave energy is lost during the breaking process, in which 30%-50% is converted to the bubble clouds to overcome the buoyancy. Hoque and Aoki[68] theoretically studied the physical mechanism of air bubble entrainment and the energy variation in wave breaking. It is found the dissipation of potential and kinetic energy are highly correlated with air bubbles entrainment.

Because of the difficulties in capturing and tracking moving bubbles or droplets (with deformation) in experiment, numerical simulation based on CFD has become prevalent in the analysis of energy dissipation[59, 69-71]. Liu et al.[65] summarized recent advances in the simulation of breaking waves and corresponding energy dissipation process. The total energy E is usually decomposed into three components according to Refs. [71-74]:

The kinetic energy

$$E_k = \frac{1}{2}\int \rho u^2 \mathrm{d}x\mathrm{d}y\mathrm{d}z \tag{1}$$

The gravitational potential energy

$$E_g = \int \rho g y \,\mathrm{d}x\mathrm{d}y\mathrm{d}z \tag{2}$$

The surface tension potential energy

$$E_s = \frac{\gamma(L-1)}{\rho_w g \lambda^2} \tag{3}$$

where γ is the surface tension coefficient, L is the arc length, λ is the wave length, ρ_w represents the liquid density. Fig. 9 shows the time evolution of different components of energy. As shown in Fig. 9(a), the total energy E_k (□) shows an abrupt decrease during the first wave period owing to a large amount of the dissipated wave energy. An exponential function $E = E_0 \mathrm{e}^{-\zeta t}$ can be well fitted for the decaying of total energy, where ζ and E_0 represents the decay rate and initial wave energy per unit width of the wave crest respectively. In the first few wave periods, the gravitational energy (∇) has been dissipated completely, while the kinetic energy (o) can remain for a longer time. The surface tension potential energy (◇) occupies very little of the total dissipated energy (less than 8%), which is similar to Iafrati's investigation[75]. Therefore, the effect of surface tensional force could be neglected in this case. Relevant studies on the energy dissipation in wave breaking provide valuable information for the analysis of energy conversion and dissipation in bow wave breaking.

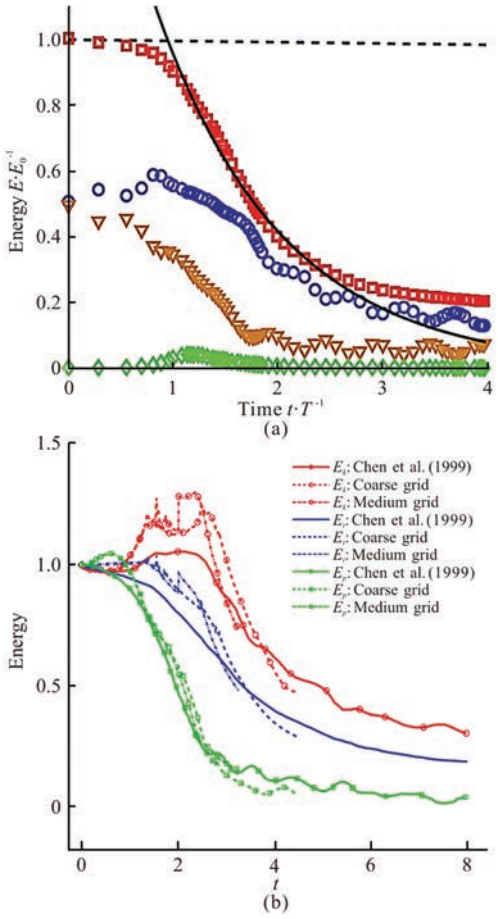

Fig. 9 (Color online) Numerically predicted energy dissipation as a function of time. (a) Time evolution of wave energy[59], (b) Total wave energy, kinetic energy, and gravitational potential energy as a function of time[66]

In terms of ship resistance, some scholars have carried out relevant studies on the added resistance due to bow wave breaking. Hong et al. established a formula to calculate the radiant energy of a three-dimensional ship hull with speed and analyze the wave-induced added resistance for three types of ships under different conditions in detail. The studies provide effective means for the prediction of added resistance of ships in wave with small amplitude. The

CFD method based on RANS equations has been widely used to investigate the added resistance of ships in wave with large steepness[76-78]. The results show that the added wave resistance present strong nonlinearity due to the free surface breaking at the wave crest. Current studies on added resistance in wave mainly focus at model scale and low sea state, the measured added resistance usually accounts for 10%-30% of the resistance in still water, indicating that wave added resistance is closely related to the water-air-bubble mixed flow. However, the component of water-air-bubble mixed flow and its effect on the ship resistance cannot be clearly explained and analyzed quantitatively in these studies. Besides, water-air-bubble mixed flow may also affect the frictional resistance due to the interaction with boundary layer flow[22], which need to be further studied and illustrated.

3. The effect of water-air-bubble mixed flow on propeller performance

For a sailing ship in the ocean, the wave breaking in the near-field wake flow and free surface deformation caused by vortical flow behind the stern will result in both significant air entrainment underwater and sweeping down of bubble clouds. Therefore, the wake flow field around the propeller contains multi-scale bubbles, which will affect the performance and efficiency of the propulsion system. The open-water tests[79-80] and traditional CFD methods have been widely applied to predict and analyze the propulsive performance[81]. These studies focused on the performance of the propellers and did not consider the wake flow behind the ship. When considering the interaction between the hull and propeller, the wake flow characteristics is quite different, which directly affect the pressure and velocity distribution of propeller. The effect of wake is usually considered by the modification of empirical coefficients. Researchers have also performed studies on the hydrodynamic behavior of propeller in viscous wake[82-83]. Pereira et al.[82] presented an experimental study of a propeller operating in a non-uniform inflow field. The non-uniformity of the wake downstream of a hull is considered by placing an array of plates as Fig. 10 showed. The pressure, noise and cavitation extension around the propeller is further studied, which could help to develop a model to predict the pressure fluctuations more accurately. Ge et al.[83] performed numerical study of cavitation and hull pressure pulses induced by a marine propeller operating in behind-hull conditions (model scale). The main focuses are the generation of tip vortex, tip vortex cavitation and the induced pressure pulses, which has been discussed in detail.

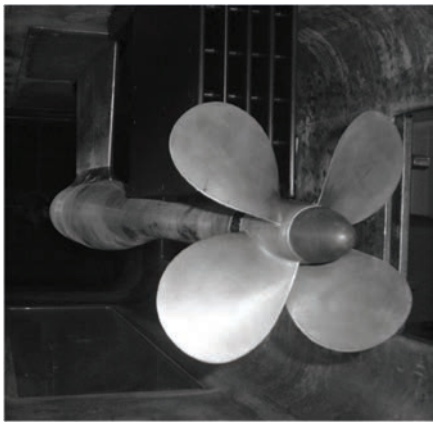

Fig. 10 The non-uniform wake generator in experiment[82]

More complicatedly, several authors[84-85] also analyzed the propulsion characteristics and separated flow field around the propeller considering the effect of complex ship 6-DOF motion and hull-propeller-rudder coupling. Although there have been considerable improvements in the prediction of propulsive performance, the wake flow in real conditions (full-scale) is not reproduced well both in experimental and simulation. One of the important reasons is that the effect of water-air-bubble mixed flow behind the stern is not included in the prediction method.

The multi-scale bubbles in water-air-bubble mixed flow near the stern is prone to cluster near the propulsion system, their effects on the propeller include two main aspects. Firstly, the sweeping down of numerous bubbles increase the non-uniformity of wake behind the hull, which will affect the propulsion performance. Some scholars have studied the open water test for propeller based on the circulating water tank and CFD results[86-87]. The propeller open water characteristics (e.g., thrust ratio KT / KT_0, torque ratio KQ / KQ_0, propeller efficiency ep/ep0) were measured with and without air bubbles relatively (Fig. 11). As showed in Fig. 11, the thrust ratio, torque ratio and propeller efficiency are all tend to decrease when the volume of air injected into the water increased. The loss of thrust and efficiency will be more than 5% and 1% respectively when the void fraction is more than 1%. Besides, the propeller pressure fluctuation on the blade is also correlated with the injected bubbles. The fluctuation is nearly twice as high as the case without bubbles if the average void fraction in the propeller disk is more than 0.2% as showed in Fig. 12.

Although the authors have concluded that the air bubbles mixing has little effect on the propeller performance both at model scale and full scale[87], the investigated module carrier is a typical vessel with wide breath and shallow draft. Therefore, the amount of air bubbles flowing into the propeller is quite small

and the position of bubble flow is above the propeller shaft as showed in Fig. 13. The complex motion of ship and enhanced air entrainment behind high-speed ship (e.g., a ship model with a transom transom[21, 88]) will obviously increase the penetration depth and injected volume of bubbles, the thrust and efficiency loss may not be neglected anymore. Advanced theory or method based on CFD or EFD results is necessary in the future to obtain a more precise prediction of propulsion performance considering the effect of large-scale water-air-bubble mixed flow.

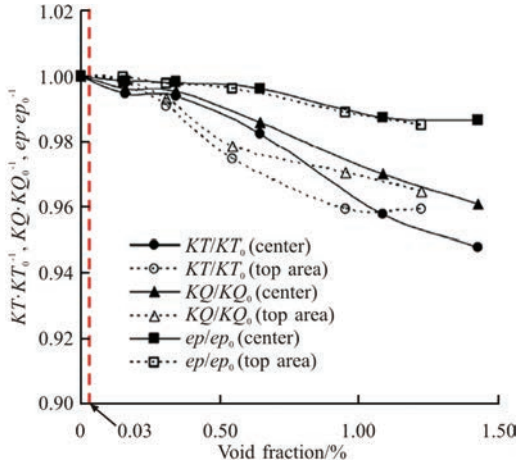

Fig. 11 (Color online) The effect of air bubbles on the propeller performance[86]

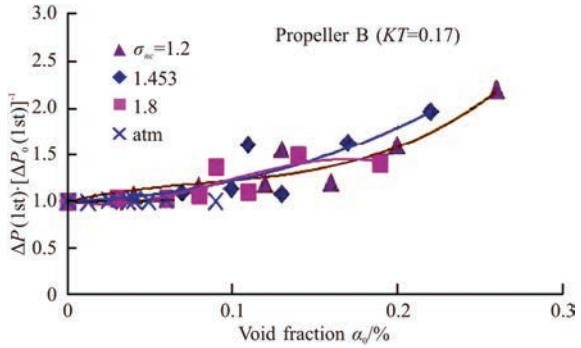

Fig. 12 (Color online) The effect of air bubbles on the propeller pressure fluctuations[86]

On the other hand, the injected bubbles will change the local pressure on the blade, which also affect the cavitation characteristics of the propeller. According to previous studies[89-91], the air content is highly correlated with incipient cavitation number. With the increase of the bubbles number and extent of aeration, the sound speed will be much less than that in single-phase water[92-93] and cavitation load on the solid surface will also decrease[94]. The cavitation number will increase[95] and the diffusion of gas will be promoted, which increases the gas content in the cavitation bubble and decrease the collapse pressure. Zhang et al.[91] believed that the strong interaction between the existed air bubbles and cavitation bubbles may change the direction of re-entrant jets and decrease the velocity of micro-jets. The collapse time will increase and thus the shock wave pressure and peak load will decrease. However, other studies think that the air bubbles will promote the formation and growth of large-scale cavitation bubbles, decrease the cavitation number. Until now, a universal and convincing understanding of the effect of air bubbles on the cavitation has not been proposed, which need to be further studied.

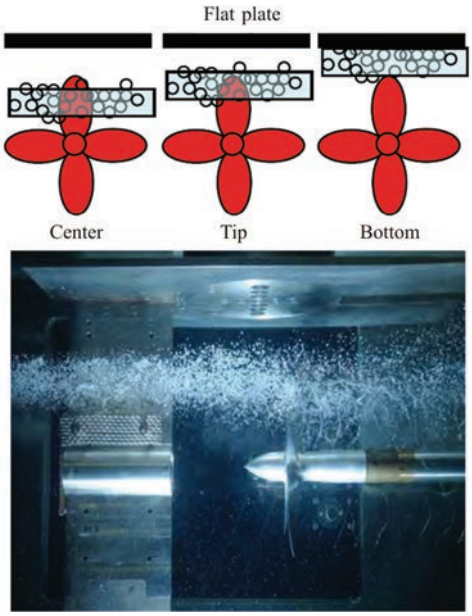

Fig. 13 (Color online) The bubble flow position (top row) and the open-water test of propeller in bubbly flow (bottom row)[87]

4. The effect of water-air-bubble mixed flow on the sea-keeping

In this section, we consider the influence of water-air-bubble mixed flow on the sea-keeping performance of ship. We are mostly concerned about the slamming characteristic caused by the violent impact between the ship and water-air-bubble mixed flow (Fig. 2(c)). This process involves the mechanic behavior with a large span of spatial and temporal scales, which brings great challenges for the experimental and numerical analysis[96]. Traditional studies provide valuable insights into the kinetic and dynamic characteristics of ship slamming. However, people mainly care about the motion and stability of ship in wave, the distribution of extreme loads and structural strength. Relevant studies considering the effects of water-air-bubbles mixing on slamming characteristics especially for discerning the physical mechanisms are rarely found.

In the previous experimental studies, vertical

wall is usually placed on the deck of ship model to mimic the deck structures and study the water-shipping event[97]. As showed in Figs. 14(a), 14(b), significant wave breaking and droplet splashing occurs due to the interaction of the shipped water with the vertical structure. Lafeber et al.[98-99] simplified the problem as the impact of breaking wave on a vertical wall structure and conducted a comparative analysis of the flow structure and impact pressure at large-scale and full-scale. It is found that the Froude-scaled measured pressure at different scales is not consistent due to the scale effect caused by water-air-bubble mixed flow. The authors have attributed the difference to the un-scaled development of building jets and compressible entrapped air[99], which has significant effects on the amplitude of local pressure peak and global force. The entrapped air cavities generated by the overturning break of wave front will alleviate the violent impact and reduce the pressure peak, which is well known as the "air cushion effect" in the water entry[100-103]. However, the evolution of entrapped air in the green water presents different behaviors, the high-pressure region will be generated by the gas entrainment and non-linear interface fragment, resulting in multiple pressure peaks on the impact point.

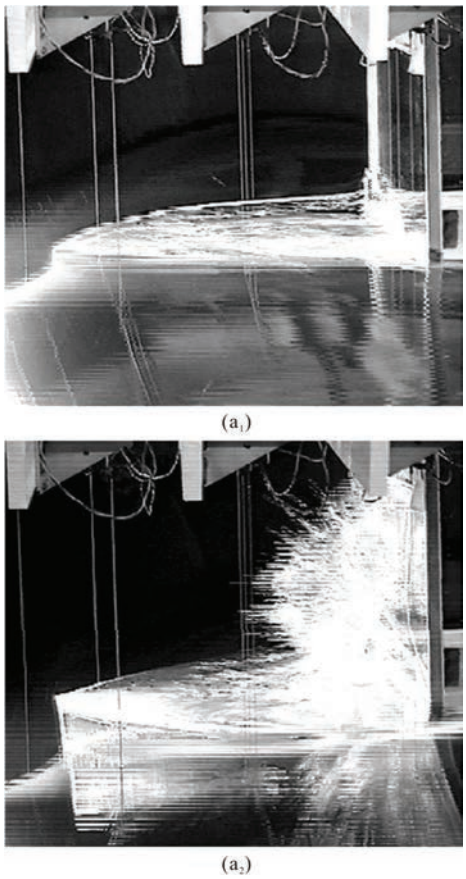

Fig. 14(a) The photographs at two subsequent instants during the interaction of the shipped water front with the vertical wall structure[97]

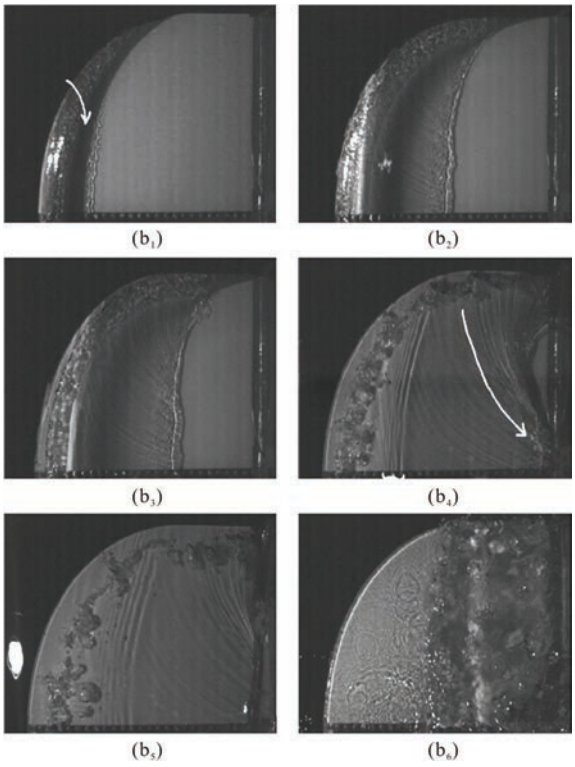

Fig. 14(b) The evolution of the water-shipping evolution[97]

In recent years, scholars have carried out a series of EFD and theoretical studies on the water-air-bubble mixed flow in the wave slamming[104-109]. The generation of spray-clouds and associated flow kinematics in the breaking wave impact on a fixed flat plate and bow-shaped models are both investigated in detail. They have depicted the important stages of wave-impact spray phenomena in Fig. 15. Firstly, the wave impact on the bow, the running-up of wave front and subsequent overturning create the water sheet. As the water sheet break-up into liquid films and big droplets, the secondary break-up will also happen. Finally, a spray cloud containing multi-scale droplets is formed, which will disperse under the wind and impact on the deck structure.

In the experiments, the bubble image velocimetry (BIV) method is employed in the highly aerated regions to measure the wave run-up velocity and digital particle image velocimetry (DPIV) method is used to measure the droplets size and velocity to clarify spray characteristics[106]. Theoretical models are established and developed step by step to predict the breakup and trajectories of droplets[109], droplet size/velocity distribution[105] and the final average droplet size within a spray cloud[107]. The spray characteristics obtained by the numerical solutions are consistent with previous field observations[110]. Smaller size droplets have a higher velocity than the medium and large droplets while they cannot reach the maximum spray heights

due to the drag force[106].

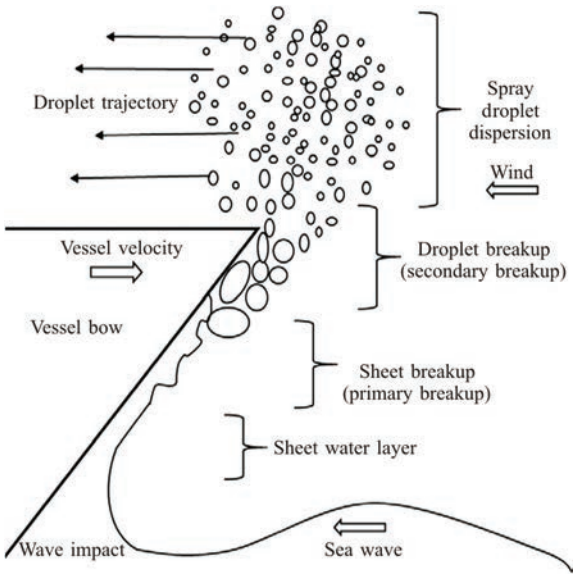

Fig. 15 The schematic diagram of the wave-impact spray phenomena[108]

For numerical studies, CFD method based on Navier-Stokes equation combined with various interface capture method has been widely used to investigate the ship slamming characteristics. The simulations can reproduce the development of large-scale motion of wave and entrapped air cavity. However, due to the present limitation of computational cost, small-scale droplets or bubbles cannot be resolved well. Therefore, the accurate spray or break-up model is necessary to capture the complete evolution of spray-clouds and analyze their effects on the slamming characteristics. Besides, the surface tension[111-112], gas/liquid compressibility[113-114] also plays important roles and should be carefully addressed in numerical model. The interface instability is highly correlated with surface tension, which may lead to drastic changes of geometrical shape of free surface[112] and affect the local slamming pressures directly. The impact load will be reduced with increasing air volume fraction[115] and gas compressibility while the pressure peak is much larger when considering the liquid compressibility[116, 119] as Fig. 16 showed.

There have also been some meshless methods to deal with the slamming of marine object[120-122]. The method can reproduce the jet and splash phenomenon with smaller computational cost[120] (as Fig. 17 presented). However, the difficulties in handling complex geometry and viscosity effects make it difficult to be applied to the study of large-scale sailing ships.

5. The effect of water-air-bubble mixed flow on the ship maneuverability

As mentioned before, numerous bubbles in the water-air-bubble mixed flow will sweep down along the hull and cluster near the propulsion system, which will affect the dynamic behavior of hull-propeller-rudder. There are three main sources of the bubbles underwater: Bubbles transported from upstream generated by bow wave and shoulder wave breaking, bubbles which are entrapped underwater due to the large-scale vortical structures in the wake flow and the bubbles generated by propeller cavitation. It is difficult to study this problem through experiment due to the complex underlying physics and great challenges in measuring the instantaneous three-dimensional flow structures. Also, it is hard to reproduce the appreciable air bubbles mixing in the model-scale due to the scale effect.

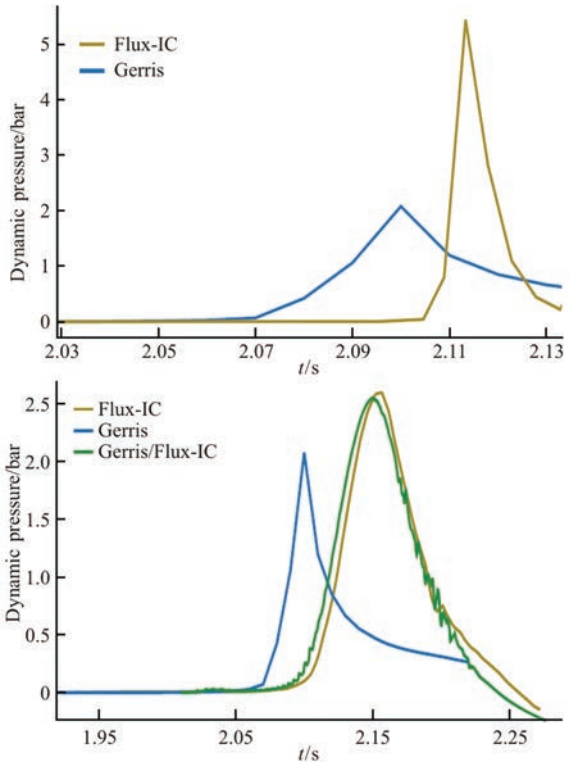

Fig. 16 (color online) Slamming pressure as a function of time for breaking wave against a vertical wall. Blue line and yellow line represent the results obtained by incompressible (Gerris[117-118]) and compressible methods respectively (Flux-IC[119])

Therefore, numerical simulation becomes a valuable tool to investigate the effects of water-air-bubbles mixed flow on the ship maneuverability. The overset grid (Fig. 18) methods have presented great advantages in dealing with the large motion of multiple objects. Therefore, it has been widely used to investigate the problem of ship maneuver in waves[85, 124] as shown in Fig. 19. However, these studies didn't consider the formation and evolution of multi-scale entrapped bubbles underwater.

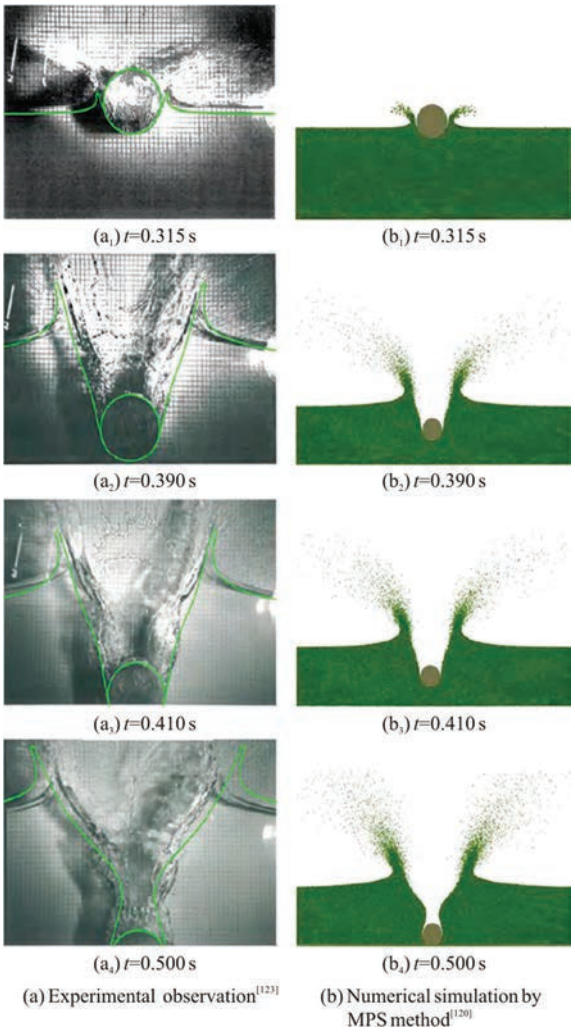

Fig. 17 (Color online) The temporal evolution splashing jets during the water entry of rigid circular cylinder. (a) Experimental observation[123], (b) Numerical simulation by MPS method[120]

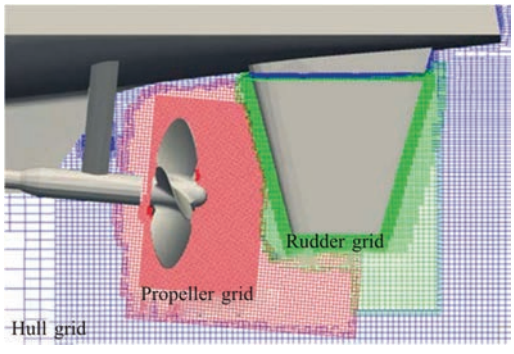

Fig. 18 (Color online) The schematic diagram of the overset girds[85]

To resolve the multi-scale bubbles in the wake flow, Drazen et al.[88] adopted a self-developed numerical flow analysis (NFA) solver for the large eddy simulation (LES) of incompressible two-phase flow[125-127]. The solver is based on the Cartesian grid system and a cut cell-typed immersed boundary method is employed to implement the boundary conditions on the hull. The authors have presented high-fidelity simulation of water-air-bubble mixed flow behind a simplified transom stern as shown in Fig. 20, analyze the air entrainment behavior and two-phase characteristics[88]. However, the model is stationary and underwater propulsion system is not considered in the simulation.

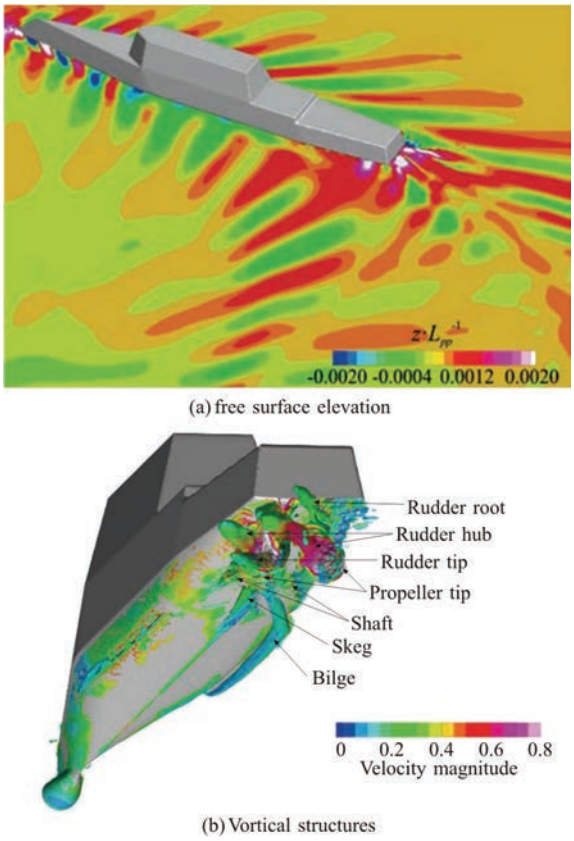

Fig. 19 (Color online) Numerical simulations of turning circle maneuver in calm water[124]. (a) Free surface elevation, (b) Vortical structures

Li et al.[31] have performed valuable numerical study of the bubbly wake during ship maneuvering (Fig. 21) based on the polydisperse two-fluid model combined with a single-phase level set method for interface capturing. The geometric model is the research vessel Athena R/V with two propellers and rudders. Sub-grid air entrainment model is included in the solution of Navier-Stokes equations[127] and the effect of compressible bubbles are also considered[128]. To improve the computational efficiency in the simulation of large-scale problems, several numerical strategies were developed for multiple dynamic behaviors of bubbles[129-130]. In the study, the bubble entrainment density and bubble transportation, size

distribution and the effects of vortical structures are under full investigation. It is noted that the void fraction and maximum penetration depth of bubbles in the wake will increase during the ship turning as Fig. 22 showed. Also, the ship maneuver enhances the bubble entrainment near the transom stern, resulting in more bubbles in the wake flow[31].

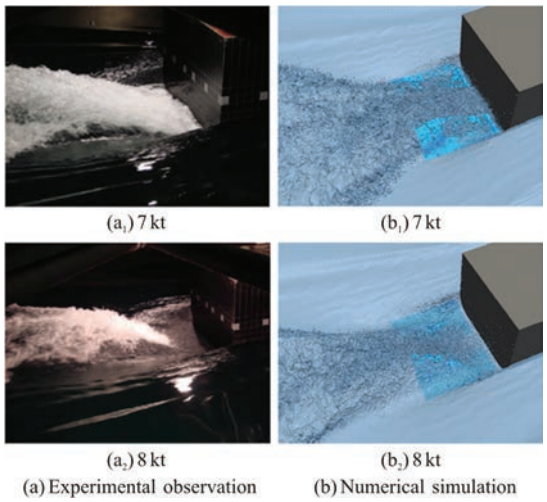

Fig. 20 (Color online) The water-air-bubble mixed flow behind the transom stern[88]. (a) Experimental observation, (b) Numerical simulation

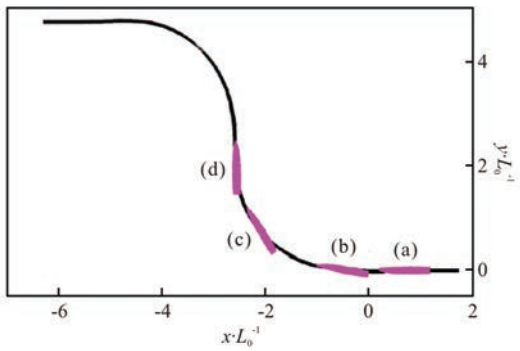

Fig. 21 (Color online) The trajectory of the ship during the maneuver[31]

Recently, some scholars preliminarily studied the effect of water-air-bubble mixed flow on the rudder force with experimental measurements and numerical simulation[131]. The results show that pulsating air bubbles will gather on the rudder surface, and their spatial distribution is correlated with the propeller rotation. The pulsating air bubbles aggravate the instability of rudder force, which may promote the rudder cavitation and reduce the rudder efficiency.

6. Conclusions and future directions

The phenomenon of water-air-bubble mixed flow is commonly found around a sailing ship at full-scale, while it is hard to be reproduced at model scale. Studies on the bubbly wake and wave breaking for a high-speed ship model have provided valuable data for understanding the formation and evolution of water-air-bubble mixed flow. However, the number of entrapped bubbles (or spray droplets) and the intensity of water-air mixture is far below that of the full-scale case. Therefore, large-scale numerical simulation considering the effect of water-air-bubble mixed flow is required, which propose demanding requirements for the accuracy and credibility of the numerical model.

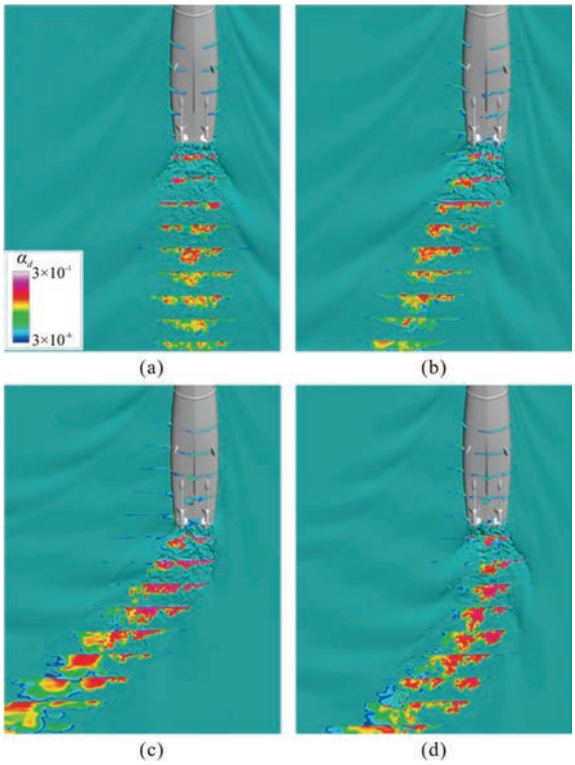

Fig. 22 (Color online) The distribution of void fraction at different cross sections in the bubbly wake during the ship maneuver[31]. The four selected picture at typical instants are corresponding with the key point in Fig. 21

In terms of the ship performance, the effect of water-air-bubble mixed flow is usually ignored in the traditional theory. However, with the urgent need of energy saving and emission reduction for sailing ships, the physical understanding and control of water-air-bubble mixed flow may provide a new way to overcome the problem. However, the current knowledge about the effect of water-air-bubble mixed flow on the ship performance is quite insufficient. Experiments or simulations based on simplified geometrical model present some qualitative conclusions. Quantitative results and systematic studies are in demand, especially for the scale effect of water-air-bubble-mixed

flow, the energy dissipation due to the motion of numerous bubbles/droplets, the cavitation of propulsion system in the presence of injected bubbles, slamming characteristics and the coupling of hull-propeller-rudder in bubbly/spray flow.

In the future, efficient means for understanding the physical nature of water-air-bubble mixed flow and their interaction with ship should be developed. People may consider the following points:

(1) With the rapid development of the HPC (high-performance computing) technologies, the complex fluid behavior in model-scale two-phase mixed flow can be reproduced well with high-resolution LES method, such as the wave breaking and near-field bubbly wake. The high-fidelity data provide a basis to better understand the mechanical nature of water-air-bubble mixed flow and develop a credible numerical model. However, the heavily computational cost limits its widespread use. Therefore, simulation with the adaptive mesh may be a better alternative, which can greatly improve the computational efficiency of massively parallel computations of two-phase mixed flow.

(2) Since the water-air-bubble mixed flow is more significant at full-scale, the full-scale CFD method that considering the dynamic behavior of multi-scale bubbles/droplets should be developed. The polydisperse two-fluid approach[24] has shown the potential in the analysis of large-scale features of water-air-bubble flow. However, the current sub-grid air entrainment model needs to be further validated by available EFD measurements or high-fidelity simulation. Some physical phenomenon that may be dominated for the behavior of small-scale flow structures, such as the non-uniform turbulent dissipation near the wall boundary, surface tension effect, should be carefully considered.

(3) For the prediction of ship performance, the consideration of water-air-bubble mixed flow bring great challenges both for numerical method and data analysis. For example, the study on the cavitation characteristics involves the phase transition, mass transfer between three phases (cavitation bubbles, entrained bubbles and liquid phase). The numerical model should describe the cavitation inception and the interaction with surrounding bubbles correctly. The relevant study of compressible multi-phase flow may provide some basic understanding for the development of physical model.

References

[1] Delacroix S., Germain G., Gaurier B. et al. Experimental study of bubble sweep-down in wave and current circulating tank: Part I–Experimental set-up and observed phenomena [J]. *Ocean Engineering*, 2016, 120: 78-87.

[2] Delacroix S., Germain G., Gaurier B. et al. Experimental study of bubble sweep-down in wave and current circulating tank: Part II-Bubble clouds characterization [J]. *Ocean Engineering*, 2016, 120: 88-99.

[3] Mallat B., Germain G., Gaurier B. et al. Experimental study of the bubble sweep-down phenomenon on three bow designs [J]. *Ocean Engineering*, 2018, 148: 361-375.

[4] Wang W., Cai G. B., Pang Y. J. et al. Bubble sweep-down of research vessels based on the coupled Eulerian-Lagrangian method [J]. *Journal of Marine Science and Engineering*, 2020, 8(12): 1040.

[5] Dong R. R., Katz J., Huang T. T. On the structure of bow waves on a ship model [J]. *Journal of Fluid Mechanics*, 1997, 346: 77-115.

[6] Roth G. I., Mascenik D. T., Katz J. Measurements of the flow structure and turbulence within a ship bow wave [J]. *Physics of Fluids*, 1999, 11(11): 3512-3523.

[7] Olivieri A., Pistani F., Wilson R. et al. Scars and vortices induced by ship bow and shoulder wave breaking [J]. *Journal of Fluids Engineering*, 2007, 129(11): 1445-1459.

[8] Wilson R. V., Carrica P. M., Stern F. URANS simulations for a high-speed transom stern ship with breaking waves [J]. *International Journal of Computational Fluid Dynamics*, 2006, 20(2): 105-125.

[9] Wang J., Wan D. Breaking wave simulations of high-speed surface combatant using OpenFOAM [C]. *Proceedings of the Eighth International Conference on Computational Methods*, Guilin, China, 2017.

[10] Carrica P. M., Wilson R. V., Stern F. Unsteady RANS simulation of the ship forward speed diffraction problem [J]. *Computers and Fluids*, 2006, 35(6): 545-570.

[11] Ren Z., Wang J., Wan D. Numerical study of the effects of grid scale on bow wave breaking [C]. *Proceedings of the Twenty-eighth International Ocean and Polar Engineering Conference*, Sapporo, Japan, 2018.

[12] Yu A., Wan D. RANS model for bow wave breaking of a KRISO Container Ship under different speeds [C]. *Proceedings of the Eleventh International Workshop on Ship and Marine Hydrodynamics, Hamburg*, Germany, 2019.

[13] Carrica P. M., Huang J., Noack R. et al. Large-scale DES computations of the forward speed diffraction and pitch and heave problems for a surface combatant [J]. *Computers and Fluids*, 2010, 39(7): 1095-1111.

[14] Broglia R., Durante D. Accurate prediction of complex free surface flow around a high speed craft using a single-phase level set method [J]. *Computational Mechanics*, 2018, 62(3): 421-437.

[15] Wang J., Ren Z., Wan D. C. Study of a container ship with breaking waves at high Froude number using URANS and DDES methods [J]. *Journal of Ship Research*, 2020, 64(4): 346-356.

[16] Wu D., Wang J., Wan D. Delayed detached eddy simulation method for breaking bow waves of a surface combatant model with different trim angle [J]. *Ocean Engineering*, 2021, 242: 110177.

[17] Ren Z., Wang J., Wan D. Numerical simulation of ship bow wave breaking using DES and RANS [C]. *Proceedings of the Ninth International Conference on Computational Methods*, Rome, Italy, 2018.

[18] Hu Y., Liu C., Hu C. et al. Numerical investigation of flow structure and air entrainment of breaking bow wave generated by a rectangular plate [J]. *Physics of Fluids*, 2021, 33(12): 122113.

[19] Francis N., Gerard D., Michel G. et al. Simple analytical relations for ship bow waves [J]. *Journal of Fluid*

Mechanics, 2008, 600: 105-132.
[20] Francis N., Gerard D., Liu H. et al. Ship bow waves [J]. *Journal of Hydrodynamics*, 2013, 25(4): 491-501.
[21] Johansen J. P., Castro A. M., Carrica P. M. Full-scale two-phase flow measurements on Athena research vessel [J]. *International Journal of Multiphase Flow*, 2010, 36(9): 720-737.
[22] Perret M., Carrica P. M. Bubble-wall interaction and two-phase flow parameters on a full-scale boat boundary layer [J]. *International Journal of Multiphase Flow*, 2015, 73: 289-308.
[23] Ma J., Oberai A. A., Hyman M. C. et al. Two-fluid modeling of bubbly flows around surface ships using a phenomenological subgrid air entrainment model [J]. *Computers and Fluids*, 2011, 52: 50-57.
[24] Castro A. M., Carrica P. M. Eulerian polydispersed modeling of bubbly flows around ships with application to Athena R/V [J]. *International Shipbuilding Progress*, 2013, 60(1-4): 403-433.
[25] Peltzer R., Griffin O., Barger W. et al. High-resolution measurement of surface-active film redistribution in ship wakes [J]. *Journal of Geophysical Research*: Oceans, 1992, 97(C4): 5231-5252.
[26] Soloviev A., Maingot C., Agor M. et al. 3D sonar measurements in wakes of ships of opportunity [J]. *Journal of Atmospheric and Oceanic Technology*, 2012, 29(6): 880-886.
[27] Kouzoubov A., Wood S., Ellem R. Acoustic imaging of surface ship wakes [C]. *Proceedings of the Forty-third International Congress on Noise Control Engineering: Improving the World Through Noise Control*, Melbourne, Australia, 2014.
[28] Shen L., Zhang C., Yue D. K. P. Free-surface turbulent wake behind towed ship models: experimental measurements, stability analyses and direct numerical simulations [J]. *Journal of Fluid Mechanics*, 2002, 469: 89-120.
[29] Fu T. C., Fullerton A. M., Ratcliffe T. et al. A detailed study of transom breaking waves [R]. Hydromechanics Department Report, West Bethesda, USA: Carderock Division, Naval Surface Warfare Center, 2009.
[30] Fu T. C., Fullerton A. M., Drazen D. et al. A detailed study of transom breaking waves: Part II [R]. Hydromechanics Department Report, West Bethesda, USA: Carderock Division, Naval Surface Warfare Center, 2009.
[31] Li J. J., Martin J. E., Carrica P. M. Large-scale simulation of ship bubbly wake during a maneuver in stratified flow [J]. *Ocean Engineering*, 2019, 173: 643-658.
[32] Hendrickson K., Weymouth G., Yue D. K. P. et al. Wake behind a three-dimensional dry transom stern. Part 1: flow structure and large-scale air entrainment [J]. *Journal of Fluid Mechanics*, 2019, 875: 854-883.
[33] Hendrickson K., Yue D. K. P. Wake behind a three-dimensional dry transom stern. Part 2. Analysis and modelling of incompressible highly variable density turbulence [J]. *Journal of Fluid Mechanics*, 2019, 875: 884-913.
[34] Chanson H. Current knowledge in hydraulic jumps and related phenomena. A survey of experimental results [J]. *European Journal of Mechanics-B/Fluids*, 2009, 28(2): 191-210.
[35] Chachereau Y., Chanson H. Free-surface fluctuations and turbulence in hydraulic jumps [J]. *Experimental Thermal and Fluid Science*, 2011, 35(6): 896-909.
[36] Xiang M., Cheung S. C. P., Tu J. Y. et al. A multi-fluid modelling approach for the air entrainment and internal bubbly flow region in hydraulic jumps [J]. *Ocean Engineering*, 2014, 91: 51-63.
[37] Mortazavi M., Le Chenadec V., Moin P. et al. Direct numerical simulation of a turbulent hydraulic jump: Turbulence statistics and air entrainment [J]. *Journal of Fluid Mechanics*, 2016, 797: 60-94.
[38] Li Z., Liu C., Wan D. Numerical investigation on air entrainment behavior and energy evolution of hydraulic jump [C]. *Proceedings of the Thirty-First International Ocean and Polar Engineering Conference*, Rhodes, Greece, 2021.
[39] Witt A., Gulliver J., Shen L. Simulating air entrainment and vortex dynamics in a hydraulic jump [J]. *International Journal of Multiphase Flow*, 2015, 72: 165-180.
[40] Witt A., Gulliver J. S., Shen L. Numerical investigation of vorticity and bubble clustering in an air entraining hydraulic jump [J]. *Computers and Fluids*, 2018, 172: 162-180.
[41] Liu C., Hu C. Block-based adaptive mesh refinement for fluid-structure interactions in incompressible flows [J]. *Computer Physics Communications*, 2018, 232: 104-123.
[42] Liu C., Hu C. An adaptive multi-moment FVM approach for incompressible flows [J]. *Journal of Computational Physics*, 2018, 359: 239-262.
[43] Macneice P., Olson K. M., Mobarry C. et al. PARAMESH: A parallel adaptive mesh refinement community toolkit [J]. *Computer physics communications*, 2000, 126(3): 330-354.
[44] Yang X., Liu C., Wan D. et al. Numerical study of the shock wave and pressure induced by single bubble collapse near planar solid wall [J]. *Physics of Fluids*, 2021, 33(7): 073311.
[45] Shu C. W. High-order finite difference and finite volume WENO schemes and discontinuous Galerkin methods for CFD [J]. *International Journal of Computational Fluid Dynamics*, 2003, 17(2): 107-118.
[46] Ghods S., Herrmann M. A consistent rescaled momentum transport method for simulating large density ratio incompressible multiphase flows using level set methods [J]. *Physica Scripta*, 2013, T155: 014050.
[47] Rudman M. A volume-tracking method for incompressible multifluid flows with large density variations [J]. *International Journal for Numerical Methods in Fluids*, 1998, 28(2): 357-378.
[48] Owkes M., Desjardins O. A mass and momentum conserving unsplit semi-Lagrangian framework for simulating multiphase flows [J]. *Journal of Computational Physics*, 2017, 332: 21-46.
[49] Raessi M., Pitsch H. Consistent mass and momentum transport for simulating incompressible interfacial flows with large density ratios using the level set method [J]. *Computers and Fluids*, 2012, 63: 70-81.
[50] Yang Y., Liu C., Wan D. Numerical study of bubbly wake flows around a transom stern [C]. *Proceedings of the Thirty-First International Ocean and Polar Engineering Conference*, Rhodes, Greece, 2021.
[51] Deane G. B., Stokes M. D. Scale dependence of bubble creation mechanisms in breaking waves [J]. *Nature*, 2002, 418(6900): 839-844.
[52] Garrett C., Li M., Farmer D. The connection between bubble size spectra and energy dissipation rates in the upper ocean [J]. *Journal of Physical Oceanography*, 2000, 30(9): 2163-2171.
[53] Mori N., Kakuno S. Aeration and bubble measurements of coastal breaking waves [J]. *Fluid Dynamics Research*, 2008, 40(7-8): 616.
[54] Tavakolinejad M. Air bubble entrainment by breaking

bow waves simulated by a 2D+T technique [D]. Doctoral Thesis, Maryland, USA: University of Maryland, 2010.
[55] Liu C., Wang J., Wan D. C. CFD computation of wave forces and motions of DTC ship in oblique waves [J]. *International Journal of Offshore and Polar Engineering*, 2018, 28(2): 154-163.
[56] Begovic E., Mancini S., Day A. et al. Applicability of CFD methods for roll damping determination of intact and damaged ship, high performance scientific computing using distributed infrastructures: Results and scientific applications derived from the Italian PON ReCaS project [M]. Sinaapore: World Scientific, 2017, 343-359.
[57] Avci A. G., Barlas B. An experimental investigation of interceptors for a high speed hull [J]. *International Journal of Naval Architecture and Ocean Engineering*, 2019, 11(1): 256-273.
[58] Kiger K. T., Duncan J. H. Air-entrainment mechanisms in plunging jets and breaking waves [J]. *Annual Review of Fluid Mechanics*, 2012, 44: 563-596.
[59] Deike L., Melville W. K., Popinet S. Air entrainment and bubble statistics in breaking waves [J]. *Journal of Fluid Mechanics*, 2016, 801: 91-129.
[60] Metcalf B., Longo J., Ghosh S. et al. Unsteady free-surface wave-induced boundary-layer separation for a surface-piercing NACA 0024 foil: Towing tank experiments [J]. *Journal of Fluids and Structures*, 2006, 22(1): 77-98.
[61] Xing T., Kandasamy M., Stern F. Unsteady free-surface wave-induced separation: analysis of turbulent structures using detached eddy simulation and single-phase level set [J]. *Journal of Turbulence*, 2007, 8: N44.
[62] Fang Z., Xiao L., Wei H. et al. Severe wave run-ups on fixed surface-piercing square column under focused waves [J]. *Physics of Fluids*, 2020, 32(6): 063308.
[63] Pogozelski E., Katz J., Huang T. The flow structure around a surface piercing strut [J]. *Physics of Fluids*, 1997, 9(5): 1387-1399.
[64] Li Z., Liu C., Wan D. et al. High-fidelity simulation of a hydraulic jump around a surface-piercing hydrofoil [J]. *Physics of Fluids*, 2021, 33(12): 123304.
[65] Liu C., Hu Y., Li Z. et al. Recent advancement of experimental and numerical investigations for breaking waves [J]. *Journal of Harbin Institute of Technology (New Series)*, 2019, 26(5): 1-16.
[66] Wang Z., Yang J., Stern F. High-fidelity simulations of bubble, droplet and spray formation in breaking waves [J]. *Journal of Fluid Mechanics*, 2016, 792: 307-327.
[67] Rapp R. J., Melville W. K. Laboratory measurements of deep-water breaking waves [J]. *Philosophical Transactions of the Royal Society of London. Series A, Mathematical and Physical Sciences*, 1990, 331(1622): 735-800.
[68] Hoque A., Aoki S. Air entrainment by breaking waves: A theoretical study [J]. *Indian Journal of Marine Sciences*, 2006, 35(1): 17-23.
[69] Zhang Y., Liu P., Qu Q. et al. Energy conversion during the crown evolution of the drop impact upon films [J]. *International Journal of Multiphase Flow*, 2019, 115: 40-61.
[70] Ma H., Liu C., Li X. et al. Deformation characteristics and energy conversion during droplet impact on a water surface [J]. *Physics of Fluids*, 2019, 31(6): 062108.
[71] Deike L., Popinet S., Melville W. K. Capillary effects on wave breaking [J]. *Journal of Fluid Mechanics*, 2015, 769: 541-569.
[72] Chen G., Kharif C., Zaleski S. et al. Two-dimensional Navier-Stokes simulation of breaking waves [J]. *Physics of Fluids*, 1999, 11(1): 121-133.
[73] Iafrati A. Air-water interaction in breaking wave events: Quantitative estimates of drops and bubbles [C]. *Proceedings of 28th Symposium on Naval Hydrodynamics*, Pasadena, California, USA, 2010.
[74] Iafrati A. Energy dissipation mechanisms in wave breaking processes: Spilling and highly aerated plunging breaking events [J]. *Journal of Geophysical Research: Oceans*, 2011, 116(C7): C07024.
[75] Iafrati A. Numerical study of the effects of the breaking intensity on wave breaking flows [J]. *Journal of Fluid Mechanics*, 2009, 622: 371-411.
[76] Sadat-Hosseini H., Wu P. C., Carrica P. M. et al. CFD verification and validation of added resistance and motions of KVLCC2 with fixed and free surge in short and long head waves [J]. *Ocean Engineering*, 2013, 59: 240-273.
[77] He W., Diez M., Zou Z. et al. URANS study of Delft catamaran total/added resistance, motions and slamming loads in head sea including irregular wave and uncertainty quantification for variable regular wave and geometry [J]. *Ocean Engineering*, 2013, 74: 189-217.
[78] Shen Z., Wan D. RANS computations of added resistance and motions of a ship in head waves [J]. *International Journal of Offshore and Polar Engineering*, 2013, 23(4): 263-271.
[79] Ebrahimi A., Razaghian A. H., Tootian A. et al. An experimental investigation of hydrodynamic performance, cavitation, and noise of a normal skew B-series marine propeller in the cavitation tunnel [J]. *Ocean Engineering*, 2021, 238: 109739.
[80] Zou D., Xu J., Zhang J. et al. The hydroelastic analysis of marine propellers considering the effect of the shaft: Theory and experiment [J]. *Ocean Engineering*, 2021, 221: 108547.
[81] Xu L., Wan D. Numerical research on hydrodynamic characteristics of propeller boss cap fins [J]. *Chinese Journal of Ship Research*, 2018, 13(S1): 15-21(in Chinese).
[82] Pereira F., Salvatore F., Di Felice F. et al. Experimental investigation of a cavitating propeller in non-uniform inflow [C]. *Proceedings of the 25th Symposium on Naval Hydrodynamics*, St. John's, Canada, 2004.
[83] Ge M., Svennberg U., Bensow R. E. Investigation on RANS prediction of propeller induced pressure pulses and sheet-tip cavitation interactions in behind hull condition [J]. *Ocean Engineering*, 2020, 209: 107503.
[84] Liu C., Wang J., Wan D. CFD simulations of self-propulsion and turning circle maneuver up to 90 degrees of ship in waves [J]. *Journal of Ship Research*, 2021, 65(2): 139-152.
[85] Wang J. H., Wan D. C. CFD Investigations of ship maneuvering in waves using naoe-FOAM-SJTU solver [J]. *Journal of Marine Science and Application*, 2018, 17(3): 443-458.
[86] Kawabuchi M., Kawakita C., Mizokami S. et al. CFD predictions of bubbly flow around an energy-saving ship with Mitsubishi air lubrication system [J]. *Mitsubishi Heavy Industries Technical Review*, 2011, 48(1): 53-57.
[87] Kawakita C. Study on marine propeller running in bubbly flow [C]. *Proceedings of the Third International Symposium on Marine Propulsors*, Launceston, Tasmania, Australia, 2013.
[88] Drazen D. A., Fullerton A. M., Fu T. C. et al. A comparison of model-scale experimental measurements and

computational predictions for a large transom-stern wave [C]. *Proceedings of the 28th Symposium on Naval Hydrodynamics*, Pasadena, California, USA, 2010.
[89] Holl J. W., Carroll J. A. Observations of the various types of limited cavitation on axisymmetric bodies [J], *Journal of Fluids Engineering*, 1981, 103(3): 415-421.
[90] Hammitt F. G. Cavitation and multiphase flow phenomena [M]. New York, USA: McGraw-Hill, 1980.
[91] Zhang F., Xu J., Xu J. et al. Overview and discussions on the advances in the mechanism studies of air entrainment against cavitation erosion [J]. *Journal of Hydroelectric Engineering*, 2010, 29(2): 7-10(in Chinese).
[92] Liu D. Y. The speed of sound in two-phase flows under the condition of velocity-equilibrium between phases [J]. *Acta Mechanica Sinica*, 1990, 22(6): 660-669.
[93] Shuai Q. H. Study of the speed of sound and compressibility on aerated flow and the critical air concentration for avoiding cavitation erosion damage [D]. Doctoral Thesis, Chengdu, China: Sichuan University, 1995(in Chinese).
[94] Huang J., Li S., Ni H. G. The effect of air entrainment on the-collapsing pressure of a cavitation bubble in a liquid [J]. *Journal of Hydraulic Engineering*, 1985, (4): 10-17(in Chinese).
[95] Peterka A. J. The effect of entrained air on cavitation pitting [C]. *Proceedings: Minnesota International Hydraulic Convention*, Minnesotu, USA, 1953.
[96] Dias F., Ghidaglia J. M. Slamming: Recent progress in the evaluation of impact pressures [J]. *Annual Review of Fluid Mechanics*, 2018, 50: 243-273.
[97] Barcellona M., Landrini M., Greco M. et al. An experimental investigation on bow water shipping [J]. *Journal of Ship Research*, 2003, 47(4): 327-346.
[98] Lafeber W., Bogaert H., Brosset L. Elementary loading processes (ELP) involved in breaking wave impacts: Findings from the Sloshel project [C]. *Proceedings of the Twenty-second International Ocean and Polar Engineering Conference*, Rhodes, Greece, 2012.
[99] Lafeber W., Bogaert H., Brosset L. Comparison of wave impact tests at large and full scale: Results from the sloshel project [C]. *Proceedings of the Twenty-Second International Ocean and Polar Engineering Conference*, Rhodes, Greece, 2012.
[100] Greco M. A. Two-dimensional study of green-water loading [D]. Doctoral Thesis, Trondheim, Norwegian: Norwegian University of Science and Technology, 2001.
[101] Chuang S. L. Experiments on flat-bottom slamming [J]. *Journal of Ship Research*, 1966, 10(1): 10-17.
[102] Chuang S. L. Experiments on slamming of wedge-shaped bodies [J]. *Journal of Ship Research*, 1967, 11(3): 190-198.
[103] Chen Z., Xiao X. Simulation analysis on the role of air cushion in the slamming of a flat-bottom structure [J]. *Journal of Shanghai Jiaotong University*, 2005, 39(5): 670-673(in Chinese).
[104] Bodaghkhani A., Dehghani S. R., Muzychka Y. S. et al. Understanding spray cloud formation by wave impact on marine objects [J]. *Cold Regions Science and Technology*, 2016, 129: 114-136.
[105] Bodaghkhani A., Colbourne B., Muzychka Y. S. Prediction of droplet size and velocity distribution for spray formation due to wave-body interactions [J]. *Ocean Engineering*, 2018, 155: 106-114.
[106] Bodaghkhani A., Dowdell J. R., Colbourne B. et al. Measurement of spray-cloud characteristics with bubble image velocimetry for braking wave impact [J]. *Cold Regions Science and Technology*, 2018, 145: 52-64.
[107] Bodaghkhani A., Muzychka Y. S., Colbourne B. An analytical model of final average droplet size prediction of wave spray cloud [J]. *International Journal of Heat and Fluid Flow*, 2018, 74: 110-117.
[108] Dehghani S. R., Muzychka Y. S., Naterer G. F. Droplet trajectories of wave-impact sea spray on a marine vessel [J]. *Cold Regions Science and Technology*, 2016, 127: 1-9.
[109] Dehghani S. R., Muzychka Y. S., Naterer G. F. Water breakup phenomena in wave-impact sea spray on a vessel [J]. *Ocean Engineering*, 2017, 134: 50-61.
[110] Ryerson C. C. Superstructure spray and ice accretion on a large US Coast Guard cutter [J]. *Atmospheric research*, 1995, 36(3-4): 321-337.
[111] Frihat M., Karimi M. R., Brosset L. et al. Variability of impact pressures induced by sloshing investigated through the concept of "singularization" [C]. *Proceedings of the Twenty-Sixth International Ocean and Polar Engineering Conference*, Rhodes, Greece, 2016.
[112] Frihat M., Brosset L., Ghidaglia J. M. Experimental study of surface tension effects on sloshing impact loads [C]. *Proceedings of Thirty-Second International Workshop on Water and Floating Bodies*, Dalian, China, 2017.
[113] Rafiee A., Dias F., Repalle N. Numerical simulations of 2D liquid impact benchmark problem using two–phase compressible and incompressible methods [C]. *Proceedings of the Twenty-Third International Offshore and Polar Engineering Conference*, Anchorage, Alaska, 2013.
[114] Rafiee A., Dutykh D., Dias F. Numerical simulation of wave impact on a rigid wall using a two-phase compressible SPH method [J]. *Iutam Symposium on Particle Methods in Fluid Dynamics*, 2015, 18: 123-137.
[115] Elhimer M., Jacques N., Alaoui A. E. et al. The influence of aeration and compressibility on slamming loads during cone water entry [J]. *Journal of Fluids and Structures*, 2017, 70: 24-46.
[116] Mrabet A. Algorithmic acceleration for the numerical simulation of wave impacts. "Roofline" type models for processor performance, application to CFD [D]. Doctoral Thesis, Paris, France: ENS Paris-Saclay, 2018(in French).
[117] Popinet S. An accurate adaptive solver for surface-tension-driven interfacial flows [J]. *Journal of Computational Physics*, 2009, 228(16): 5838-5866.
[118] Popinet S. Gerris: A tree-based adaptive solver for the incompressible Euler equations in complex geometries [J]. *Journal of Computational Physics*, 2003, 190(2): 572-600.
[119] Braeunig J. P., Desjardins B., Ghidaglia J. M. A totally Eulerian finite volume solver for multi-material fluid flows: Enhanced natural interface positioning (ENIP) [J]. *European Journal of Mechanics-B/Fluids*, 2009, 28(4): 475-485
[120] Chen X., Wan D. GPU accelerated MPS method for large-scale 3-D violent free surface flows [J]. *Ocean Engineering*, 2019, 171: 677-694.
[121] Chen X., Wan D. Numerical simulation of three-dimensional violent free surface flows by GPU-Based MPS method [J]. *International Journal of Computational Methods*, 2019, 16(4): 1843012.
[122] Zhang Y., Tang Z., Wan D. Numerical investigations of waves interacting with free rolling body by modified MPS method [J]. *International Journal of Computational Methods*, 2016, 13(4): 1641013.

[123] Greenhow M., Lin W. M. Nonlinear-free surface effects: Experiments and theory [R]. Cambridge, USA: Massachusetts Institute of Technology, 1983.
[124] Wang J., Zhao W., Wan D. Free maneuvering simulation of ONR Tumblehome using overset grid method in naoe-FOAM-SJTU solver [C]. *Proceedings of the 31th Symposium on Naval Hydrodynamics*, Monterey, USA, 2016.
[125] Dommermuth D. G., O'shea T. T., Wyatt D. C. et al. An application of cartesian-grid and volume-of-fluid methods to numerical ship hydrodynamics [C]. *Proceedings of the Ninth International Conference on Numerical Ship Hydrodynamics*, Ann Arbor, Michigan, USA, 2007.
[126] Brucker K., O'shea T., Dommermuth D. et al. Numerical simulations of breaking waves–weak spilling to strong plunging [C]. *Proceedings of the 28th Symposium on Naval Hydrodynamics*, Pasadena, California, USA, 2010.
[127] Castro A. M., Li J., Carrica P. M. A mechanistic model of bubble entrainment in turbulent free surface flows [J]. *International Journal of Multiphase Flow*, 2016, 86: 35-55.
[128] Li J., Carrica P. M. An approach to couple velocity/pressure/void fraction in two-phase flows with incompressible liquid and compressible bubbles [J]. *International Journal of Multiphase Flow*, 2018, 102: 77-94.
[129] Li J., Castro A. M., Carrica P. M. A pressure-velocity coupling approach for high void fraction free surface bubbly flows in overset curvilinear grids [J]. *International Journal for Numerical Methods in Fluids*, 2015, 79(7): 343-369.
[130] Castro A. M., Carrica P. M. Bubble size distribution prediction for large-scale ship flows: Model evaluation and numerical issues [J]. *International Journal of Multiphase Flow*, 2013, 57: 131-150.
[131] Quang P. K., Van Duy V., Tung T. X. et al. Study on synchronous effects of free surface and propeller rotation on vessel rudder force [C]. *IOP Conference Series: Earth and Environmental Science*, 2020, 527(1): 012009.